Exp Brain Res (2011) 210:595–606
DOI 10.1007/s00221-011-2591-5

RESEARCH ARTICLE

Cross-axis adaptation improves 3D vestibulo-ocular reflex alignment during chronic stimulation via a head-mounted multichannel vestibular prosthesis

Chenkai Dai · Gene Y. Fridman · Bryce Chiang · Natan S. Davidovics · Thuy-Anh Melvin · Kathleen E. Cullen · Charles C. Della Santina

Received: 1 December 2010 / Accepted: 31 January 2011 / Published online: 4 March 2011

Abstract By sensing three-dimensional (3D) head rotation and electrically stimulating the three ampullary branches of a vestibular nerve to encode head angular velocity, a multichannel vestibular prosthesis (MVP) can restore vestibular sensation to individuals disabled by loss of vestibular hair cell function. However, current spread to afferent fibers innervating non-targeted canals and otolith end organs can distort the vestibular nerve activation pattern, causing misalignment between the perceived and actual axis of head rotation. We hypothesized that over time, central neural mechanisms can adapt to correct this misalignment. To test this, we rendered five chinchillas vestibular deficient via bilateral gentamicin treatment and unilaterally implanted them with a head-mounted MVP. Comparison of 3D angular vestibulo-ocular reflex (aVOR) responses during 2 Hz, 50°/s peak horizontal sinusoidal head rotations in darkness on the first, third, and seventh days of continual MVP use revealed that eye responses about the intended axis remained stable (at about 70% of the normal gain) while misalignment improved significantly by the end of 1 week of prosthetic stimulation. A comparable time course of improvement was also observed for head rotations about the other two semicircular canal axes and at every stimulus frequency examined (0.2–5 Hz). In addition, the extent of disconjugacy between the two eyes progressively improved during the same time window. These results indicate that the central nervous system rapidly adapts to multichannel prosthetic vestibular stimulation to markedly improve 3D aVOR alignment within the first week after activation. Similar adaptive improvements are likely to occur in other species, including humans.

Keywords Vestibular nerve · Vestibular prosthesis · Vestibular implant · Vestibulo-ocular reflex, VOR, labyrinth · Bilateral vestibular deficiency · Areflexia · Adaptation · Electrical stimulation

C. Dai · G. Y. Fridman · B. Chiang · N. S. Davidovics · T.-A. Melvin · C. C. Della Santina (✉)
Departments of Otolaryngology—Head & Neck Surgery and Biomedical Engineering, Vestibular NeuroEngineering Laboratory, Johns Hopkins University School of Medicine, Ross Bldg Rm 830, 720 Rutland Ave., Baltimore, MD 21205, USA
e-mail: charley.dellasantina@jhu.edu

K. E. Cullen
Department of Physiology, McGill University, Montreal, QC, Canada

Introduction

Normally, the three semicircular canals (SCC) of each vestibular labyrinth sense head rotation. The SCCs within each labyrinth are mutually orthogonal, so hair cells in a given canal sense only one component of three-dimensional (3D) head angular velocity. Vestibular afferents innervating those hair cells transmit this information to central pathways in the brainstem and cerebellum to control the 3D angular vestibulo-ocular reflex (aVOR), which maintains stable vision by driving extraocular muscles to produce eye movements opposite the direction of head rotation. Sensory input from the vestibular labyrinths also drives postural reflexes and contributes to perception of head movement and orientation.

Loss of input from both vestibular labyrinths can lead to chronic disequilibrium, postural instability, and decreased visual acuity due to illusory movement of the world during head motion (Grunbauer et al. 1998; Minor 1998; Gillespie and Minor 1999). Several ear disorders, including ototoxic

drug exposure, ischemia, infection, genetic abnormality, and trauma to the inner ears, can all cause bilateral loss of vestibular sensation. Currently, the only clinical treatment with demonstrated success in ameliorating profound bilateral vestibular deficiency is vestibular rehabilitation; individuals who fail to improve with rehabilitative exercises remain disabled.

A multichannel vestibular prosthesis (MVP) that delivers electrical stimuli to the three ampullary branches of a vestibular nerve to encode signals from gyroscopes that sense head 3D rotational velocity can help stabilize gaze and normalize perception of head movement. We have described such a device and demonstrated its ability to partly restore the 3D aVOR (Della Santina et al. 2005, 2007, 2010; Fridman et al. 2010; Davidovics et al. 2010), using an approach similar to that initially described by Cohen and Suzuki (e.g., Cohen et al. 1964; Suzuki and Cohen 1964) and later adapted to a single-channel head-mounted prosthesis prototype by Gong, Merfeld, Lewis and colleagues (e.g., Gong and Merfeld 2000, 2002; Merfeld et al. 2006, 2007; Lewis et al. 2010). Clinical experience and experimental data from animals suggest that restoring function to one labyrinth is a reasonable goal as long as the unilaterally implanted device can encode both excitatory and inhibitory head rotations, because individuals with a single normal labyrinth typically compensate well for the lack of sensation from the other side (Curthoys and Halmagyi 1995; Black et al. 1996; Cullen 2008). However, despite promising results, current spread and imprecision of electrode placement can reduce MVP effectiveness as a result of spurious activation of non-target axons and consequent misalignment between the actual and perceived axis of head motion (Della Santina et al. 2007; Fridman et al. 2010; Davidovics et al. 2010).

The central nervous system can adapt to improve aVOR alignment when there is discordance between the head rotation axis encoded by vestibular nerve input and the axis of aVOR movements necessary to stabilize gaze. Most experiments examining this effect have relied on paradigms in which a visual surround is artificially rotated or tilted about one axis while a normal subject is rotated about another axis. For example, cats pitched up and down about the interaural axis while viewing an optokinetic drum rotating about a superoinferior axis exhibit "cross-axis adaptation" such that subsequent head pitch in darkness elicits an aVOR response with a large yaw component (Schultheis and Robinson 1981, Baker et al. 1986, 1987; Harrison et al. 1986). Similar effects have been observed in monkeys exposed to a synchronously moving visual surround during head rotation (Fukushima et al. 1996; Angelaki and Hess 1998) or surgical transposition of extraocular muscles (Leinfelder and Black 1941). Humans exposed to a tilted visual surround develop changes in perception of spatial orientation (Mikaellan and Held 1964; Morant and Beller 1965, Ebenholtz 1966; Mack and Rock 1968) and aVOR responses (Callan and Ebenholtz 1982) appropriate to reduce retinal image slip and tilt. In each of these studies, adaptive changes became evident within a few hours of exposure to the altered visual condition and improved, but did not completely eliminate, aVOR misalignment.

Complementing studies in which normal individuals are subjected to abnormal visual conditions, several studies have examined changes in aVOR gain and/or alignment after partial or complete unilateral vestibular deafferentation (e.g., Aw et al. 1996; Lasker et al. 2000; Della Santina et al. 2002; Sadeghi et al. 2006, 2010). After such a lesion, aVOR gain for ipsilesional head rotations initially drops and then partially recovers over time (Sadeghi et al. 2010). Aw et al. (1996) demonstrated that long after unilateral vestibular injury or selective semicircular canal occlusion, aVOR misalignment persists for high-acceleration transient head rotations but is minimal for less dynamic stimuli typical of most daily activities. In other words, the central nervous system appears able to correct for aVOR misalignment except under exceptionally challenging conditions.

Whether the brain can similarly compensate for the misalignment that initially results from current spread and suboptimal MVP electrode placement remains an open question with important clinical implications. In the present study, we quantified the time course and ultimate extent of cross-axis adaptation to prosthetically evoked vestibular nerve activity. Two prior studies have shown that aVOR eye movements evoked in squirrel monkeys by a single-channel head-mounted prosthesis after lateral canal plugging revealed that aVOR gain, eye movement axis, and symmetry changed over the course of 7–60 days of prosthesis use to result ultimately in aVOR responses that were better aligned (in 2 dimensions) but still abnormally low in gain (Lewis et al. 2002, 2010). One possible explanation for why aVOR adaptation to prosthetic stimuli in those studies was apparently slower and less complete than that observed in studies of normal subjects exposed to altered visual input could be that prosthetic stimuli elicit artificial patterns of vestibular afferent activity that are so different from normal that they present a great challenge to brainstem circuits that mediate cross-axis aVOR adaptation. Notably, the prosthetic stimuli applied in these previous studies would have elicited artificial patterns of vestibular afferent activity that differ markedly from those encountered in everyday life. In particular, the strategy employed by Lewis et al. used a single channel of motion sensing and stimulation (so that all 5 of the remaining SCCs presumably presented the vestibular nuclei with input incongruent with the actual head rotation). In addition, both studies

used baseline prosthetic stimulation pulse rates of 200–250 pulses/s (i.e., when the head is stationary), which are about twice the normal resting rate in vestibular afferents in squirrel monkeys.

We hypothesized that an alternative strategy in which vestibular nerve activity is evoked using a multichannel device that not only encodes 3D head movement but also modulates stimulation rates around a baseline rate close to normal could engender post-activation improvements in 3D aVOR gain and alignment similar to those observed in visual-vestibular conflict study subjects with normal labyrinthine function. To test this hypothesis, we fitted five vestibular-deficient chinchillas with a head-mounted MVP and periodically assayed the gain and 3D axis of aVOR eye movement responses during whole-body passive rotations in darkness about the mean axis of each SCC pair. Comparison of aVOR eye responses measured on the first, third, and seventh days of continual MVP use to responses without MVP stimulation and to normative data revealed that cross-axis adaptation considerably improves 3D aVOR alignment during the first week of chronic stimulation.

Methods

Experimental subjects and design

Five wild-type adult female chinchillas (450–600 g) were used for all experiments, which were performed in accordance with a protocol approved by the Johns Hopkins Animal Care and Use Committee, which is accredited by the Association for the Assessment and Accreditation of Laboratory Animal Care (AAALAC) International.

Prior to experimentation, all animals were rendered bilaterally vestibular deficient via intratympanic gentamicin treatment and canal plugging using techniques described below. Electrodes were then implanted in each of the SCCs of the left ear and connected to a percutaneous plug on top of the head. A head post was rigidly affixed to allow fixation and accurate orientation of the skull during subsequent testing. Prior to the onset of chronic, motion-modulated prosthetic stimulation, aVOR eye movement responses to sinusoidal head rotations in darkness with the prosthesis firing at baseline rates on each channel (not modulating with head movement) were measured using a 3D video-oculography (VOG) system adapted from one previously described in detail (Migliaccio et al. 2005; Migliaccio et al. 2010). These initial test sessions were carried out 5–8 weeks after surgery and gentamicin treatment, and data reported for head movement stimuli during constant-rate stimulation were acquired 3–5 h after the prosthesis was turned on (in non-modulation mode). During each testing session, aVOR eye movements were recorded in response to head rotation at 0.2, 0.5, 1, 2, and 5 Hz (peak velocity 50°/s) about the yaw (horizontal), left anterior/right posterior (LARP) and right anterior/left posterior (RALP) rotational axes, as determined within approximately ±5° using external skull landmarks and intraoperative observation of SCC orientation (Hullar and Williams 2006).

The MVP was then mounted atop the chinchilla's head with its gyroscope axes aligned parallel to the corresponding mean SCC axes. Prostheses were constantly powered for 7 days during which animals resided in their usual housing facility under diurnal lighting conditions between test sessions. For each animal, 3D aVOR eye movement responses of one or both eyes to sinusoidal head rotation were measured on the first, third, and seventh days of prosthetic stimulation, with no interim changes in prosthesis settings. Upon the completion of the last session, aVOR responses were measured a final time 4–48 h after the prosthesis power was turned off.

Surgical procedures

We implanted intralabyrinthine electrodes in the left labyrinth of each chinchilla using surgical techniques described previously (Della Santina et al. 2007; Fridman et al. 2010). With an animal under general inhalational anesthesia (isoflurane, 3–5%) supplemented by a field block (1% lidocaine/1:100 K epinephrine, plus 0.25% bupivicaine), we positioned a head post on the skull at the midline, perpendicular to the skull at the bregma so that when the animal was later positioned in the experimental apparatus, the mean horizontal semicircular canal plane would be perpendicular to the Earth-vertical axis of a rotating table. We positioned electrodes for stimulation of the anterior ampullary nerve via a fenestration in the nerve's canal just medial of the anterior canal ampulla. We positioned electrodes for stimulation of the horizontal branch of the ampullary nerve via a ~100-μm fenestration on the anterolateral wall of the horizontal ampulla. We inserted electrodes for stimulation of the posterior branch of the ampullary nerve via a fenestration in the thin segment of the posterior canal and advanced them toward the ampulla until encountering a slight resistance indicating the electrode tip had reached a sharp bend in the posterior canal that prior dissections have revealed as a constant feature near that canal's crista.

Two reference electrodes were implanted to provide an option of "steering" current injected by an active stimulating electrode near a crista. A "far reference" electrode with a large surface area was implanted in the neck musculature, and a "near reference" electrode was positioned in the labyrinth's common crus via the anterior SCC fenestration.

At the time of left labyrinth implantation, the three SCCs in right ear were plugged with bone chips and fascia; however, we did not plug the three canals in the left ear. (This minimized the risk of damaging the membranous labyrinth beyond whatever injury was caused by electrode implantation alone, allowing these animals to serve in a separate study of how electrode implantation impacts natural SCC head motion sensitivity.) To ablate the animal's vestibular hair cell sensitivity to head movement, both ears were treated postoperatively via intratympanic injection of ~0.5 mL gentamicin solution (26.7 mg/mL buffered to pH 7.4 with sodium bicarbonate) using a protocol described previously (Hirvonen et al. 2005; Della Santina et al. 2005a, b). All surgical procedures and gentamicin treatment were completed 5–8 weeks prior to the start of the experiments described in this report, so that vestibular compensation to fixed deficits caused by these interventions should have reached a steady state.

A percutaneous connector to the stimulating and the reference electrodes was positioned on top of the head next to the head post. The connector, electrodes, and post were embedded in dental acrylic (ESPE ProTemp II, 3 M Corp., Minneapolis, MN), forming a rigid connection to the skull.

Prosthetic stimulation paradigm

Prior to commencing the adaptation trial, we measured 3D aVOR responses to head rotation in darkness with the MVP on but firing only at baseline rates that did not modulate with head motion. We then programmed the MVP to sense 3D head angular velocity and accordingly modulate the pulse rate of charge balanced, symmetric, biphasic current pulses delivered to each canal's ampullary nerve. We determined the stimulation current amplitude for each electrode by gradually increasing the current amplitude of 200 μs/phase symmetric constant-current biphasic pulse trains modulated between 0 and 400 pulse/s (pps) at 1 Hz while we measured 3D eye velocity using real-time 3D VOG as described below. For adaptation experiments, we set the stimulus current for each electrode at the level that evoked maximum eye velocity without eliciting signs of facial nerve activation. This typically corresponded to a stimulus current amplitude at which the 3D axis of aVOR responses for stimulation on a given SCC's electrode on day 1 was not perfectly aligned with that SCC's axis.

After we identified the optimal electrode current amplitude and set it as a constant for each stimulation channel, we determined a "mapping function" for each SCC, by which head angular velocity about that SCC's axis would be transformed into changes in stimulus pulse frequency. To do this, we first measured peak-positive aVOR-evoked eye velocity as a function of "stimulus intensity" (SI), defined by the same convention we have used in prior studies (Fridman et al. 2010; Davidovics et al. 2010): 100% SI implies full-range modulation of pulse frequency, to 400 pulses/s for leftward (excitatory) head velocities >300 deg/s, to 0 pps for rightward (inhibitory) head velocities >300 deg/s, and baseline stimulation at 60 pps when the head is still. SI of X% implies excitatory modulation up to [60 + (400−60)·X%] pps and inhibitory modulation to [60−60·X%] pps. We used 60-pps baseline stimulation rate to mimic the mean resting rate of the normal chinchilla vestibular afferent fibers (Baird et al. 1988; Hullar et al. 2005); the mean resting rate after intratympanic gentamicin treatment is typically about 60% of normal (Hirvonen et al. 2005; Della Santina et al. 2005a, b). Because the baseline was not midway between minimum and maximum rates, the relationship between head velocity and pulse rate necessarily included a lower sensitivity (pps/deg-s^{-1}) for inhibitory head rotations than for excitatory head rotations. To characterize the dependence of eye responses on SI, we measured responses for different SI stepped in 20% SI increments from 60 pps baseline to 400 pps maximum pulse rate (i.e., 128, 196, 264, 332, 400 pps) and from 60 pps baseline to 0 pps minimum pulse rate (i.e., 48, 36, 24, 12, 0 pps, respectively). We then used these data to construct a "map" determining the desired SI level the prosthesis should present to a SCC for any given head velocity (i.e., gyro signal level) about that SCC's axis.

We mounted the prosthesis in a case atop the head post, taking care to align all three gyroscopes with their respective mean SCC planes. To power the prosthesis, we used three 3.4 V lithium ion batteries in parallel so that batteries could be replaced without interrupting power delivery. We housed the batteries in a vest that fit snugly around the animal's chest but did not restrict movement or respiration.

Eye movement recording and analysis

During each testing session, eye movements were recorded during sinusoidal head rotations in darkness at 0.2, 0.5, 1, 2, and 5 Hz and peak velocity 50°/s about the horizontal, LARP, and RALP axes. We used a real-time, binocular 3D VOG system to record eye movements (Migliaccio et al. 2005, 2010; Della Santina et al. 2007; Fridman et al. 2010). Recordings from each eye indicating horizontal, vertical, and torsional eye rotations in eye coordinates were converted to 3D rotational position in rotation vector form in a right-hand-rule canal-referenced coordinate system. For responses to sinusoidal stimuli, each of the three eye movement components (horizontal, LARP, and RALP) were separately averaged for >5 cycles free of saccades and blinks. LARP and RALP axes were approximated as being 45° off the midline and in the mean plane of the horizontal SCCs. For each component of each response and

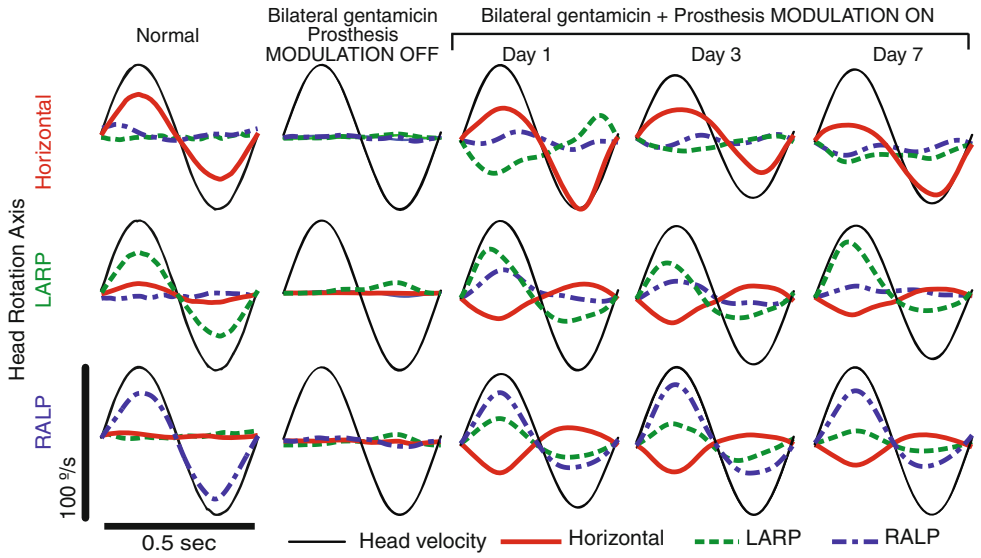

Fig. 1 Responses to head rotation before, during, and after 1 week of prosthetic stimulation using a multichannel vestibular prosthesis. *Column 1* Head rotational velocity (black) and mean eye rotational velocity components (horizontal, left anterior/right posterior [LARP], and right anterior/left posterior [RALP]) of a normal chinchilla during 2 Hz, 50°/s peak whole-body rotations in darkness. *Top, middle, and bottom rows* show *data* during whole-body rotations about the horizontal, LARP, and RALP axes, respectively, adapted from Della Santina et al. 2007. *Column 2* Head and eye velocity measured 4 weeks after electrode implantation and bilateral gentamicin treatment in a chinchilla, with the prosthesis set to fire at constant rates (mean 60 pulse/s on each channel) that are not modulated by head rotation. *Columns 3–5* Head and eye velocity measured on the first, third, and seventh days of continuous motion-modulated prosthetic stimulation. Note the progressive (though still incomplete) reduction in wrong-axis eye movement components. Each trace is the mean of ≥5 cycles; SD < 5°/s at each time point for each trace. The first half-cycle in each *plot* is the response to excitation of the left labyrinth

for each stimulus trace, we used a single-frequency Fourier analysis to compute the magnitude of the best-fit sinusoid under the constraint that the response frequency was the same as the known stimulus frequency. When responses exhibit asymmetry between excitatory and inhibitory half-cycles, this computation results in a magnitude approximating the average between that, which would result from fitting to either half-cycle alone. When data were available for both eyes, the mean 3D axis reported is the mean of the right eye, while disconjugacy is reported as the angle between the 3D rotation axes of the left and right eye. To determine whether eye/head gain and misalignment changed significantly between test sessions, we used a multivariate general linear model constructed and analyzed using SPSS 16.0 software (SPSS Inc., Chicago IL), with $P < 0.05$ considered significant.

Results

When a normal chinchilla is rotated sinusoidally at 2 Hz, 50°/s peak in darkness, the eyes respond by moving in the direction opposite the rotation of the head at approximately half of the velocity of the head motion (Fig. 1, column 1; see also Migliaccio et al. 2010). A chinchilla treated bilaterally with gentamicin and plugging of the semicircular canals on the right side exhibits no aVOR response during head rotation with prosthetic stimuli firing only at constant baseline rates when the prosthesis is set to ignore head rotation signals reported by the its gyro sensors (Fig. 1, column 2). Eye movement responses recorded during head rotation on day 1 of motion-modulated MVP stimuli (within 6 h of initial MVP activation) are already aligned somewhat with head rotation axes, but significant misalignment is evident in the form of non-zero response components about axes other than the axis of head rotation (Fig. 1, column 3). For example, when the animal's head is rotated about the horizontal axis, the eyes respond primarily by rotating about the horizontal axis, but a substantial LARP component is present as well (Fig. 1, column 3, top). On the third and seventh days after MVP activation, the LARP component of the eye response is substantially attenuated, while the horizontal component remains nearly constant in its response to horizontal head rotation (Fig. 1, columns 3 and 4, top). A similar improvement in misalignment is evident on the third and the seventh days of stimulation when this animal is tested by rotating it about the LARP and the RALP axes (Fig. 1, middle and bottom rows, respectively). This progressive improvement in misalignment is illustrated for a second animal in Fig. 2, which shows how the mean 3D axis of eye rotation evolves over 7 days of prosthesis use, with aVOR eye responses to head rotations about each of the three mean anatomic SCC axes approaching ideal eye responses over time.

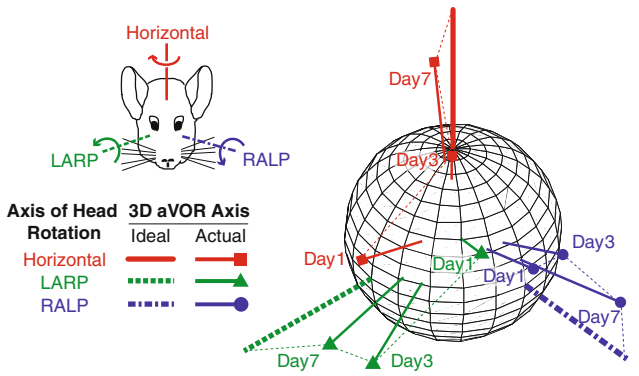

Fig. 2 Changes in axis of eye response for one chinchilla over 7 days of stimulation. Each *data* vector depicts the 3D axis and magnitude of aVOR responses during whole-body 2 Hz, 50°/s peak head rotations in darkness about the mean horizontal, LARP, and RALP semicircular canal axes. Vector length indicates the peak response velocity; for comparison, thick axes depict inverse of 50°/s peak head rotations about each canal axis. *Data* shown are for peak excitatory responses; curved arrows in inset show direction of aVOR response to excitation of the corresponding semicircular canal in the left labyrinth. Progression over time toward the ideal response is apparent for each axis of head rotation

This improvement over time in encoding of head movement axis was evident for all five animals studied, for all three axes of head rotation tested. Figure 3 shows the amplitude of each eye rotation component during sinusoidal 2 Hz, 50°/s peak horizontal (first column), LARP (second column), and RALP (third column) whole-body head rotations in darkness for each of the 5 animals individually, and Fig. 4 summarizes these data averaged over all five animals. The mean component of 3D eye rotation about the head rotation axis (i.e., the desired response) remains nearly constant for the first, third, and seventh days of continual prosthesis use, while the relative amplitude of each (undesired) mean off-axis component progressively and consistently decreases, so that responses on day 7 of prosthetic stimulation are much more similar to normal responses than on day 1 (two-way ANOVA with factors animal and day 1 vs day 7: $P = 0.014$ for yaw head rotation, 0.044 for LARP, 0.019 for RALP). To ensure that this marked improvement was not due to the recovery of hair cell function, we measured responses again with the prosthesis power turned off on day 7. Without prosthesis stimulation, aVOR responses were again consistent with profound bilateral hypofunction, confirming that all responses and improvement observed during the 7-day trial depended on prosthetic input.

Improvement in aVOR alignment was also evident for every stimulus frequency examined. Figure 5 shows the aVOR misalignment angle and gain for different frequencies and axes of head rotation averaged for the right eye in each of five animals. For each of the frequencies tested, the gain of the eye responses remains relatively high and constant (Fig. 5 row 1), while misalignment between the 3D aVOR response and the axis of head rotation improves over the 7 days of prosthetic stimulation (Fig. 5 row 2;

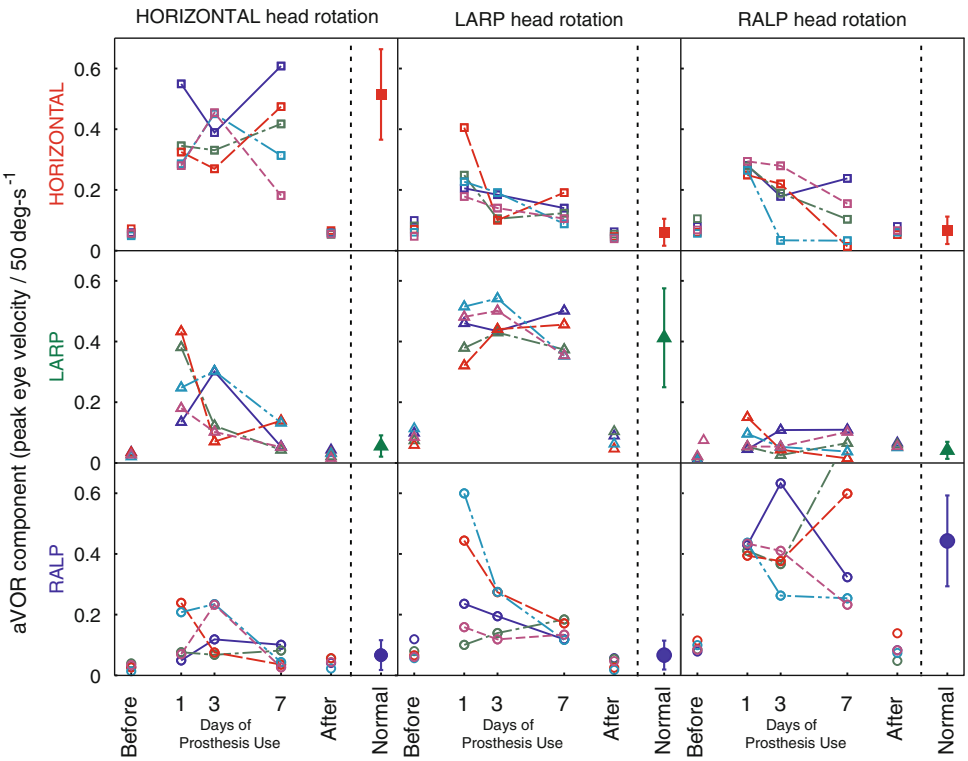

Fig. 3 Gain of each component of 3D aVOR responses for each of $N = 5$ chinchillas during 2 Hz, 50°/s peak whole-body rotations about the horizontal, LARP, and RALP canal axes on the first, third, and seventh days of continuous stimulation using a head-mounted multichannel vestibular prosthesis. Before values measured to head movement with the prosthesis stimulating at constant pulse rates, independent of head velocity, 3–5 h after prosthesis activation. *After* values measured 4–48 h after the prosthesis was powered off on day 7. *Normal* Responses of 5 normal chinchillas

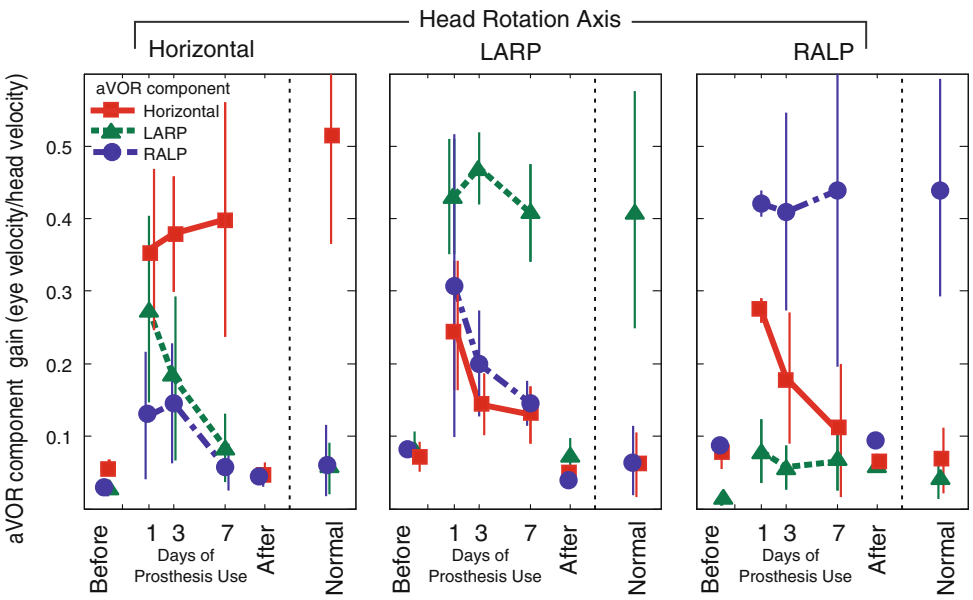

Fig. 4 Mean ± SD gain ($N = 5$ chinchillas) for each component of the peak 3D aVOR eye movement response during 2 Hz, 50°/s peak whole-body rotations about the horizontal, LARP, and RALP canal axes on the first, third, and seventh days of continuous stimulation using a head-mounted multichannel vestibular prosthesis. *Before* values measured to head movement with the prosthesis stimulating at constant pulse rates, independent of head velocity, 3–5 h after prosthesis activation. *After* values measured 4–48 h after the prosthesis was powered off on day 7. *Normal* Responses of 5 normal chinchillas

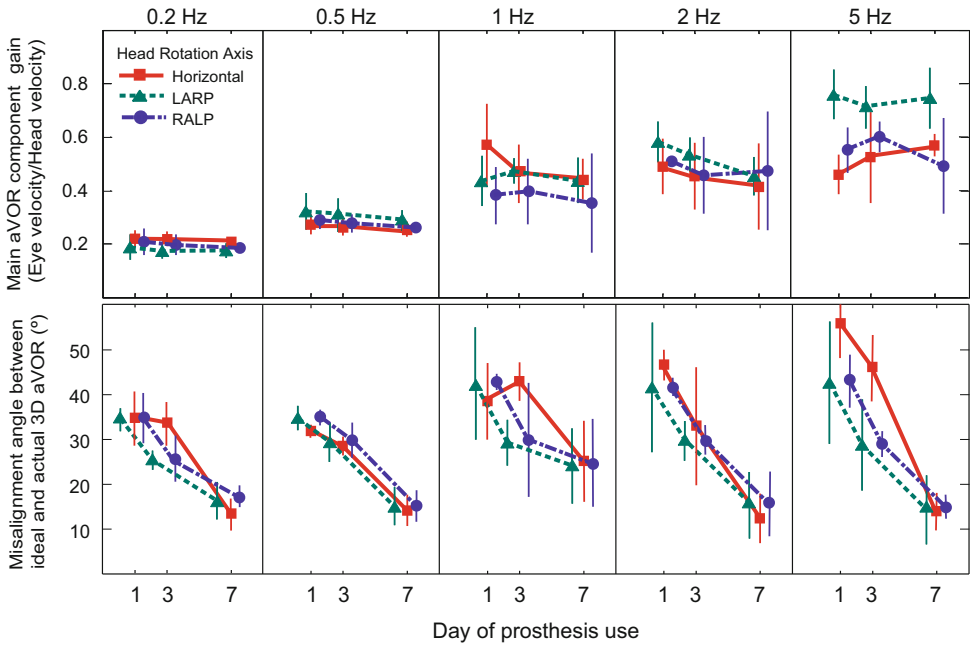

Fig. 5 Mean ± SD gain (*top*) and eye/head misalignment angle (*bottom*) for $N = 5$ chinchillas, displayed for each component of the peak 3D aVOR eye movement response during 50°/s peak whole-body rotations in darkness at 0.2–5 Hz about the horizontal, LARP, and RALP canal axes on the first, third, and seventh days of continuous stimulation using a head-mounted multichannel vestibular prosthesis. The 3D aVOR response maintained gain of the desired component while improving misalignment over 7 days of continuous prosthesis for every stimulus frequency, axis, and animal examined

ANOVA: $P < 0.05$ for day 1 vs day 7 for every head rotation axis and frequency combination). This pattern was consistent for every animal.

Improvement in aVOR binocular alignment (i.e., reduction in disconjugacy between the two eyes) was also evident. Figure 6 shows the mean ± SD interocular misalignment angle for all five animals, as assessed during sinusoidal 2 Hz, 50°/s peak horizontal (first column), LARP (second column), and RALP (third column) whole-body head rotations in darkness. $N \geq 3$ for each point in Fig. 6, because binocular data were not available for every animal/axis/day combination. For each axis of head rotation tested, mean misalignment between the 3D aVOR response axes of the two eyes reduced significantly over the 7 days of prosthetic stimulation (ANOVA: $P < 0.05$ for day 1 vs day 7 for every head rotation axis).

Discussion

During 1 week of continuously wearing a head-mounted 3D multichannel vestibular prosthesis, animals previously rendered vestibular deficient via gentamicin treatment rapidly adapted toward a well-aligned 3D aVOR with gains close to normal. Although the ultimate 3D axes of eye rotation did not align perfectly with head rotation,

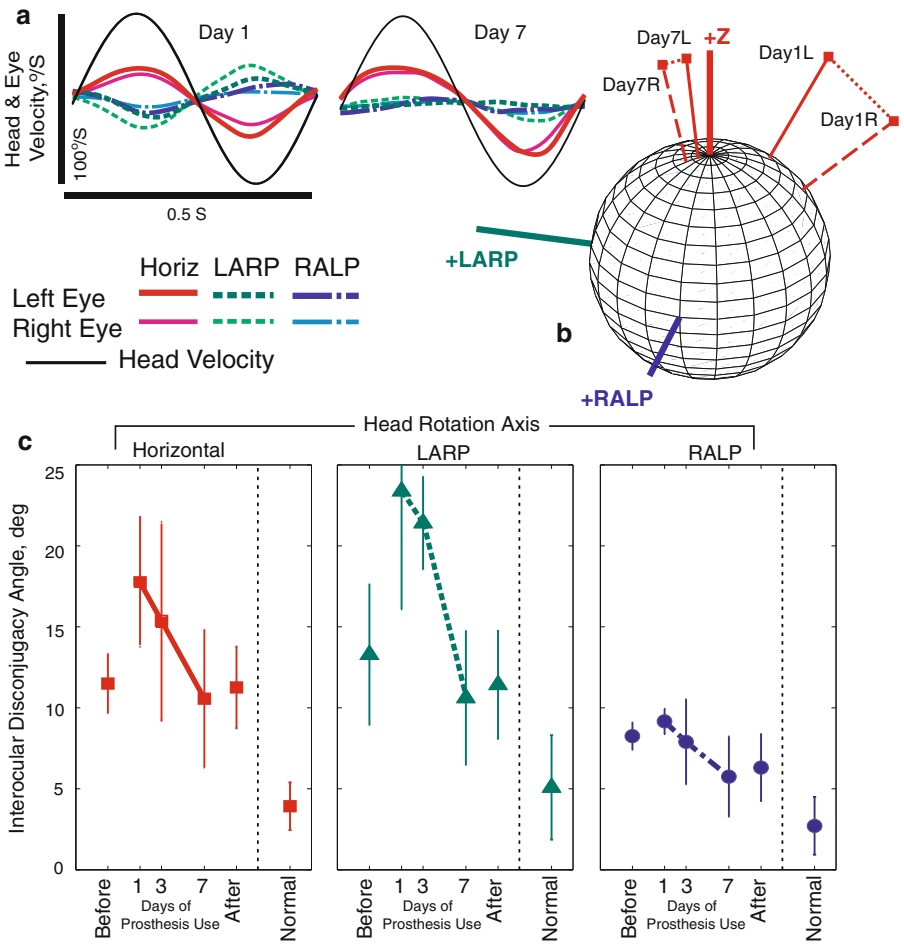

Fig. 6 Changes in disconjugacy during adaptation to prosthetic stimulation. **a** Head rotational velocity and mean eye rotational velocity components (horizontal, LARP, and RALP) for each eye of a normal chinchilla during 2 Hz, 50°/s peak whole-body rotations in darkness about the mean horizontal semicircular canal axis on days 1 and 7 of continual prosthesis use. For each component of eye rotation, differences between the two eyes are reduced by day 7. **b** 3D aVOR response axes corresponding to *data* in *Panel A*. *L* left eye, *R* right eye. By day 7, responses for both eyes align better with each other and to the horizontal head rotation axis (+Z). **c** Mean ± SD disconjugacy angle (between the 3D axes of rotation for the two eyes) during 2 Hz whole-body 50°/s peak sinusoidal head rotations in darkness about the horizontal (*filled square*), LARP (*filled triangle*) and RALP (*filled circle*) semicircular canal axes. Disconjugacy of the aVOR response improved over 7 days of continuous prosthesis. Each *data* point for prosthesis animals is the mean of 3–5 cases; $N = 5$ for normal animals

misalignment improved significantly in every animal for every frequency and every axis of head rotation examined. Subsequent testing without prosthetic input confirmed that the performance improvements we observed over time were not due to recovery of labyrinthine hair cell function. Instead, animals apparently recruited central adaptive mechanisms analogous to those that mediate cross-axis adaptation in normal animals and humans exposed to synchronous but orthogonally directed visual and vestibular stimuli (Schultheis and Robinson 1981; Baker et al. 1986; Harrison et al. 1986; Fukushima et al. 1996; Angelaki and Hess 1998; Peng et al. 1994; Trillenberg et al. 2003).

In some respects, the experimental paradigm we employed is analogous to the typical visual-vestibular conflict paradigm used in those prior studies of cross-axis adaptation. Both create a visual-vestibular discordance to drive neural plasticity and ultimately reduce misalignment between visual and vestibular inputs. However, rather than exposing subjects to artificial and abnormal visual scene motion that is incongruent with normal vestibular input, our paradigm exposed subjects to artificial and abnormal vestibular inputs (the distorted pattern of vestibular nerve activation elicited by imperfectly selective prosthetic stimulus currents) that engender a net vestibular percept incongruent with normal visual input.

Notably, the animals in this study experienced a pattern of vestibular nerve input that was markedly distorted, even when compared with the abnormal visual inputs experienced by subjects in studies of optically induced cross-axis

adaptation. For example, in addition to 3D visual-vestibular misalignment that can be velocity- and axis dependent, the vestibular nerve activity pattern evoked by multichannel prosthetic stimulation also includes abnormally synchronous spike timing across most or all active fibers, abnormally regular spiking intervals, and inadvertent activation of macular nerves in patterns that no real head movement should ever elicit. Moreover, only the implanted labyrinth receives any signal that varies with head rotation, while the contralateral labyrinth effectively reports that the head is stationary. Considering the extent to which the resultant vestibular nerve input patterns differ from normal, spontaneous correction of most misalignment over just 1 week is a striking demonstration of the vestibular nervous system's adaptive ability. In contrast, individuals who undergo cochlear implantation adapt to comparably distorted cochlear nerve activation pattern over a much longer time (typically 3–6 months for young post-lingually deafened adults to approach an apparent plateau of performance; Chatelin et al. 2004).

Correction of multimodal cross talk due to aberrant macular nerve stimulation

While the improvement we observed in disconjugacy between the two eyes could simply be a by-product of each eye's 3D aVOR becoming better aligned with the head's axis of rotation, it could instead represent an active process of adaptation whereby central neuronal networks suppress responses to aberrant macular nerve input. Focal mechanical stimulation of one or more ampullary nerves causes binocular eye movements with little or no disconjugacy (e.g., during nystagmus due to benign paroxysmal positional vertigo or superior semicircular canal dehiscence in otherwise normal subjects [Cremer et al. 2000]), so we would expect inadvertent electrical stimulation of non-target ampullary nerves to elicit aVOR responses that are conjugate regardless of how well they align with the head rotation axis. In contrast, existing evidence suggests that the eye movement responses to activation of a single region on a single macula (or other combinations of axons within the utricular and saccular nerves) are disconjugate (Suzuki et al. 1969a, b; Fluur and Mellström 1970a, b, 1971; Goto et al. 2003, 2004; Curthoys 1987). It seems reasonable to assume that the disconjugacy we observed between 3D rotation axes of the two eyes in each animal upon initial MVP activation represents an electrically evoked translational VOR (tVOR) and/or ocular tilt reaction driven by inadvertent macular nerve stimulation. Improvement in that disconjugacy suggests an active motor learning process by which the vestibular central nervous system corrects for aberrant multimodal sensory cross talk between head angular velocity and linear acceleration.

Although we did not quantitatively assess tVOR responses to translational accelerations in the present study, an obvious lack of a normal ocular counter roll to tilt in these animals after gentamicin treatment suggests that their natural tVOR is minimal or absent. Because we did not command the MVP to measure or encode gravitational or translational acceleration in these experiments, any spurious excitation of the utricular and saccular nerves would have been in phase with head angular rotation rather than changes in the head's gravito-inertial linear acceleration.

We did not quantitatively characterize animals' head tilt, gait, indicators of spatial orientation perception, or other non-aVOR behaviors dependent on labyrinthine input. However, we did observe signs suggesting that all of these improve along with 3D aVOR performance. Each animal developed a pronounced head tilt (non-prosthesis ear down) immediately upon prosthesis baseline pulse rate activation. By the end of 1 week of prosthesis use, the head tilt had completely resolved in each animal. After that, powering the device off elicited a pronounced prosthesis ear down head tilt, limb extension on the non-prosthesis side, and circling gait toward the prosthesis side, as would be observed after destruction of the remaining normal labyrinth after an animal is fully compensated following unilateral labyrinthectomy.

Comparison with prior studies of prosthetic aVOR alignment

Using a one channel head-mounted vestibular prosthesis aligned with the horizontal or posterior SCC, Lewis et al. (2002, 2010) found that alternating between high- and low-sensitivity mappings of head velocity to pulse rate improved both the gain (from 0.11 to 0.17) and 2D misalignment toward the desired responses to yaw head rotations (i.e., a $\sim 30°$ shift from mostly pitch to mostly yaw; roll was not measured) over 20–60 days of continual prosthesis use. Although direct comparison between the present study's 3D results in chinchillas and the Lewis et al. studies' 2D results in monkeys is complicated by species and stimulation protocol differences, it appears that the time course of 3D aVOR realignment was expedited in chinchillas receiving 3-channel MVP stimulation, such that it was consistent with previous studies of cross-axis adaptation in normal animals (e.g., Schulteis and Robinson 1981) and gain adaptation in labyrinthectomized animals (e.g., Sadeghi et al. 2010).

One reason for the apparently greater speed of misalignment reduction in the present study compared with that of Lewis et al. (2002, 2010) could be that normal chinchillas have a better aligned 3D aVOR than do normal monkeys (Migliaccio et al. 2010). A second reason could be that while the MVP we used stimulated each of three

ampullary nerves with pulse frequency modulation about baseline rates similar to those of normal chinchilla vestibular afferents, Lewis et al. used a single-channel device with baseline stimulation rates 2–2.5 × higher than the natural spontaneous rates of normal rhesus afferents (200–250 pps when compared with 100 spikes/s in rhesus). Such high baseline rates may be so different from normal that they drive vestibular nucleus and cerebellar neurons outside the physiologic range within which they normally operate to correct for misalignment. In brain slice and whole-brain preparations, artificially high afferent firing rates engender long-term depression in vestibular nucleus neurons that normally mediate adaptive corrections in aVOR gains (du Lac et al. 2010; Malinvaud et al. 2010).

Changes in 3D aVOR asymmetry

The goal of using supernormal baseline rates is to achieve symmetric responses for excitatory and inhibitory head rotations using a unilaterally implanted prosthesis. By first adapting an animal to high baseline pulse rates, one can then downmodulate stimulus pulse rates below baseline to encode inhibitory head rotations (e.g., see Lewis et al. 2010; Della Santina et al. 2007). By using more nearly normal baseline rates in the MVP for the present study, we accepted a greater degree of aVOR asymmetry in exchange for a larger dynamic range of eye rotations in response to excitatory head rotations. We wondered whether this asymmetry would evolve as the 3D aVOR axis improved.

The asymmetry we observed during 50°/s peak, 0.2–5 Hz head rotations on days 1–7 of chronic MVP stimulation in chinchillas was similar to that exhibited by rhesus monkeys (Sadeghi et al. 2010), squirrel monkeys (Lasker et al. 2000), and humans (Furman et al. 1989) tested using similar head rotations during the first week of vestibular compensation following acute unilateral surgical deafferentation. It did not change significantly during the week of prosthesis use (e.g., see Fig. 1). Whether the improvements we observed in 3D aVOR alignment over the first week of unilateral MVP use will be accompanied by improvement in aVOR asymmetry over a longer duration of MVP use remains to be seen.

Opportunities for further study of 3D aVOR cross-axis adaptation

The anatomy of pathways mediating the 3D aVOR is well described, and the neuronal basis of 2D cross-axis aVOR adaptation has been studied as it relates to optically induced coupling (e.g., between horizontal and vertical eye movements); however, the neuronal circuits and mechanisms mediating 3D cross-axis adaptation and correction of multimodal cross talk have not yet been described in detail (reviewed in Leigh and Zee 2006). While a key goal of MVP development is to address the needs of individuals disabled by loss of semicircular canal sensation, the MVP could also serve as a scientific tool that can facilitate studies clarifying the behavior of neural circuits that mediate cross-axis 3D VOR adaptation. For example, by physically reorienting an MVP's gyro sensor array with respect to the head post, one can approximate the otherwise impossible experiment of reorienting the implanted labyrinth's SCCs with respect to the head. By virtually reorienting the relative gyro/SCC orientation via software changes, this disruption of the sensory coordinate frame of reference can be made quickly and repeatedly in any direction and to varying degrees, allowing efficient characterization of cross-axis adaptation performance under a wide array of conditions.

One topic of relevance both to clinical implementation of a MVP and to scientific study of neural mechanisms underlying adaptation and motor learning is the question of a "catchment region" for motor learning in the 3D aVOR: How close must one be to a normal vestibular nerve activation pattern for adaptive processes to reconstitute a well-aligned 3D aVOR? While studies of normal subjects subjected to incongruent vestibular and visual input report relatively modest cross-axis coupling when the starting misalignment between visual and vestibular sensations is large (e.g., Schultheis and Robinson 1981; Peng et al. 1994), evidence from 1D studies of aVOR gain suggests that adaptation occurs more quickly and achieves a more durable result when the goal is adjusted incrementally from its starting state toward the desired condition. (Schubert et al. 2008) Central neuronal mechanisms mediating 3D aVOR directional plasticity might also perform best when the starting degree of aVOR misalignment is not too great (Trillenberg et al. 2003). Although the limits of the catchment region from within which adaptive mechanisms can correct misalignment to zero is not yet known, our data and those of Schulteis and Robinson (1981) suggest that misalignment up to 90° can be corrected at least partially.

Conclusion

Multiple technological refinements can be employed to help minimize 3D aVOR misalignment on the first day of MVP activation, including optimization of electrode geometry, surgical technique, and multipolar "current steering" paradigms (Chiang et al. 2010); stimulus timing and waveform shape (Davidovics et al. 2010); and computational transformations to correct for cross talk (Fridman et al. 2010). However, the vestibular nerve activation pattern elicited by a MVP will never be normal, so some 3D aVOR misalignment at the time of initial MVP

activation is unavoidable. Our results show that adaptive neural mechanisms markedly improve 3D aVOR alignment and conjugacy over 1 week of prosthesis use, even when the starting misalignment is large and the pattern of vestibular nerve activation is profoundly abnormal. These findings in chinchillas strongly suggest that similar improvements should occur in other species, including humans.

Acknowledgments We thank Lani Swarthout for assistance with animal care. This work was funded by NIH NIDCD grants R01DC009255, K08DC6216, R01DC2390, and 5F32DC009917. CDS, GYF, and BC are inventors on pending and awarded patents relevant to prosthesis technology, and CDS holds an equity interest in Labyrinth Devices LLC.

References

Angelaki DE, Hess BJ (1998) Visually induced adaptation in three-dimensional organization of primate vestibuloocular reflex. J Neurophysiol 79(2):791–807

Aw ST, Halmagyi GM, Haslwanter T, Curthoys IS, Yavor RA, Todd MJ (1996) Three-dimensional vector analysis of the human vestibuloocular reflex in responseto high-acceleration head rotations. II. responses in subjects with unilateral vestibular loss and selective semicircular canal occlusion. J Neurophysiol 76(6):4021–4030

Baird RA, Desmadryl G, Fernandez C, Goldberg JM (1988) The vestibular nerve of the chinchilla 2. Relation between afferent response properties and peripheral innervation patterns in the semicircular canals. J Neurophysiol 60:182–203

Baker J, Harrison RE, Isu N, Wickland C, Peterson B (1986) Dynamics of adaptive change in vestibulo-ocular reflex direction. II. Sagittal plane rotations. Brain Res 371(1):166–170

Baker JF, Wickland C, Peterson B (1987) Dependence of cat vestibulo-ocular reflex direction adaptation on animal orientation during adaptation and rotation in darkness. Brain Res 408:339–343

Black FO, Wade SW, Nashner LM (1996) What is the minimal vestibular function required for compensation? Am J Otol 17:401–409

Callan JW, Ebenholtz SM (1982) Directional changes in the vestibular ocular response as a result of adaptation to optical tilt. Vision Res 22:37–42

Chatelin V, Kim EJ, Driscoll C, Larky J, Polite C, Price L, Lalwani AK (2004) Cochlear implant outcomes in the elderly. Otol Neurotol 25(3):298–301

Chiang B, Fridman GY, Della Santina CC (2010) Design and performance of a multichannel vestibular prosthesis that restores semicircular canal sensation in macaques. *IEEE Trans Neural Systems and Rehab Eng* (in press)

Cohen B, Suzuki J, Bender MB (1964) Eye movements from semicircular canal nerve stimulation in cat. Annals Otol Rhin Laryng 73:153–169

Cremer PD, Minor LB, Carey JP, Della Santina CC (2000) Eye movements in patients with superior canal dehiscence syndrome align with the abnormal canal. Neurology 55(12):1833–1841

Cullen KE (2008) Procedural learning: VOR. In: H. Eichenbaum (ed) Memory systems, vol. 3 of Learning and memory: a comprehensive reference (J.Byrne ed). Elsevier, Oxford, pp. 383–402

Curthoys IS (1987) Eye movements produced by utricular and saccular stimulation. Aviat Space Environ Med 58(9):192–197

Curthoys IS, Halmagyi GM (1995) Vestibular compensation: A review of the oculomotor, neural, and clinical consequences of unilateral vestibular loss. J Vestib Res 5(2):67–107

Davidovics NS, Fridman GY, Chiang B, Della Santina CC (2010) Effects of biphasic current pulse frequency, amplitude, duration and interphase gap on eye movement responses to prosthetic electrical stimulation of the vestibular nerve. IEEE Trans Neural Syst Rehab Eng (in press, PubMed PMID: 20813652)

Della Santina CC, Cremer PD, Carey JP, Minor LB (2002) Comparison of head thrust test with head autorotation test reveals that the vestibulo-ocular reflex is enhanced during voluntary head movements. Arch Otol Head Neck Surg. 128(9):1044–1054

Della Santina CC, Migliaccio AA, Patel AH (2005a) Electrical stimulation to restore vestibular function development of a 3-D vestibular prosthesis. Conf Proc IEEE Eng Med Biol Soc 7:7380–7385

Della Santina CC, Migliaccio AA, Park HJ, Anderson IW, Jiradejvong P, Minor LB and Carey JP (2005) 3D Vestibuloocular reflex, afferent responses and crista histology in chinchillas after unilateral intratympanic gentamicin. *Abstract 813, ARO Midwinter Meeting Proceedings*

Della Santina CC, Migliaccio AA, Patel AH (2007) A multichannel semicircular canal neural prosthesis using electrical stimulation to restore 3-D vestibular sensation. IEEE Trans Biomed Eng 54:1016–1030

Della Santina CC, Migliaccio AA, Hayden R, Melvin TA, Fridman GY, Chiang B, Davidovics NS, Dai C, Carey JP, Minor LB, Anderson ICW, Park H, Lyford-Pike S, Tang S (2010) Current and future management of bilateral loss of vestibular sensation–An update on the Johns Hopkins Multichannel Vestibular Prosthesis Project. Cochlear Implants International 11(s2):2–11

du Lac S et al (2010) Signaling and plasticity of vestibular nerve synapses onto functionally distinct vestibular nucleus neurons. Abstract 535 ARO Midwinter Meeting Proceedings

Ebenholtz SM (1966) Adaptation to a rotated visual field as a function of degree of optical tilt and exposure time. J Exp Psychol 72:629–634

Fluur E, Mellström A (1970a) Utricular stimulation and oculomotor reactions. Laryngoscope 80:1701–1712

Fluur E, Mellström A (1970b) Saccular stimulation and oculomotor reactions. Laryngoscope 80:1713–1721

Fluur E, Mellström A (1971) The otolith organs and their influence on oculomotor movements. Exp Neurol 30:139–147

Fridman GY, Davidovics NS, Dai C, Della Santina CC (2010) Vestibulo-ocular reflex responses to a multichannel vestibular prosthesis incorporating a 3D coordinate transformation for correction of misalignment. JARO 11(3):367–381

Fukushima K, Fukushima J, Chin S et al (1996) Cross axis vestibulo-ocular reflex induced by pursuit training in alert monkeys. Neurosci Res 25:255–265

Furman JM, Wall C, Kamerer DB (1989) Earth horizontal axis rotational responses in patients with unilateral peripheral vestibular deficits. Ann Otol Rhinol Laryngol 98(7 Pt 1):551–555

Gillespie MB, Minor LB (1999) Prognosis in bilateral vestibular hypofunction. Laryngoscope 109:35–41

Gong WS, Merfeld DM (2000) Prototype neural semicircular canal prosthesis using patterned electrical stimulation. Annals Biomed Eng 28:572–581

Gong WS, Merfeld DM (2002) System design and performance of a unilateral horizontal semicircular canal prosthesis. IEEE Trans Biomed Eng 49:175–181

Goto F, Meng H, Bai R, Sato H, Imagawa M, Sasaki M, Uchino Y (2003) Eye movements evoked by the selective stimulation of the utricular nerve in cats Auris Nasus Larynx 30(4):341–348

Goto F, Meng H, Bai R, Sato H, Imagawa M, Sasaki M, Uchino Y (2004) Eye movements evoked by selective saccular nerve stimulation in cats. Auris Nasus Larynx 31(3):220–225

Grunbauer WM, Dieterich M, Brandt T (1998) Bilateral vestibular failure impairs visual motion perception even with the head still. Neuroreport 9(8):1807–1810

Harrison REW, Baker JF, Isu N, Wickland CR, Peterson BW (1986) Dynamics of adaptive change in vestibulo-ocular reflex direction I. Rotations in the horizontal plane. Brain Res 371:162–165

Hirvonen TP, Minor LB, Hullar TE, Carey JP (2005) Effects of intratympanic gentamicin on vestibular afferents and hair cells in the chinchilla. J Neurophysiol 93(2):643–655

Hullar TE, Williams CD (2006) Geometry of the semicircular canals of the chinchilla (*Chinchilla laniger*). Hear Res 213(1–2):17–24

Hullar TE, Della Santina CC, Hirvonen T, Lasker DM, Carey JP, Minor LB (2005) Responses of irregularly discharging chinchilla semicircular canal vestibular-nerve afferents during high-frequency head rotations. J Neurophysiol 93:2777–2786

Lasker DM, Hullar TE, Minor LB (2000) Horizontal vestibuloocular reflex evoked by high-acceleration rotations in the squirrel monkey. III. Responses after labyrinthectomy. J Neurophysiol 83:2482–2496

Leigh RJ, Zee DS (2006) The neurology of eye movements. Oxford University Press, Oxford

Leinfelder PJ, Black NM (1941) Experimental transposition of the extraocular muscles in monkeys. Am J Ophthalmol 24:1115–1120

Lewis RF, Gong WS, Ramsey M, Minor L, Boyle R, Merfeld DM (2002) Vestibular adaptation studied with a prosthetic semicircular canal. J Vestib Res 12:87–94

Lewis RF, Haburcakova C, Gong W, Makary C, Merfeld DM (2010) Vestibuloocular reflex adaptation investigated with chronic motion-modulated electrical stimulation of semicircular canal afferents. J Neurophysiol 103(2):1066–1079

Mack A, Rock I (1968) A re-examination of the Stratton effect: egocentric adaptation to a rotated visual image. Percept Psychophys 4:57–62

Malinvaud D, Vassias I, Reichenberger I, Rossert C, Straka H (2010) Functional organization of vestibular commissural connections in frog. J Neurosci 30(9):3310–3325

Merfeld DM, Gong WS, Morrissey J, Saginaw M, Haburcakova C, Lewis RF (2006) Acclimation to chronic constant-rate peripheral stimulation provided by a vestibular prosthesis. IEEE Trans Biomed Eng 53(11):2362–2372

Merfeld DM, Haburcakova C, Gong W, Lewis RF (2007) Chronic vestibulo-ocular reflexes evoked by a vestibular prosthesis. IEEE Trans Biomed Eng 54(6):1005–1015

Migliaccio AA, MacDougall HG, Minor LB, Della Santina CC (2005) Inexpensive system for real-time 3-dimensional video-oculography using a fluorescent marker array. J Neurosci Meth 143(2):141–150

Migliaccio AA, Minor LB, Della Santina CC (2010) Adaptation of the vestibulo-ocular reflex for forward-eyed foveate vision. J Physiol 588(20):3855–3867

Mikaellan H, Held R (1964) Two types of adaptation to an optically-rotated visual field. Am J Psychol 77:257–262

Minor LB (1998) Gentamicin-induced bilateral vestibular hypofunction. JAMA 279:541–544

Morant RB, Beller HK (1965) Adaptation of prismatically rotated visual fields. Science 148:530–531

Peng GC, Baker JF, Peterson BW (1994) Dynamics of directional plasticity in the human vertical vestibulo-ocular reflex. J Vestib Res 4(6):453–460

Sadeghi SG, Minor LB, Cullen KE (2006) Dynamics of the horizontal vestibuloocular reflex after unilateral labyrinthectomy: response to high frequency, high acceleration, and high velocity rotations. Exp Brain Res 175(3):471–484

Sadeghi S, Minor LB, Cullen KE (2010) Neural correlates of motor learning: dynamic regulation of multimodal integration in the macaque vestibular system. J Neurosci 30(30):10158–10168

Schubert MC, Della Santina CC, Shelhamer M (2008) Incremental angular vestibulo-ocular reflex adaptation to active head rotation. Exp Brain Res 191(4):435–446

Schultheis LW, Robinson DA (1981) Directional plasticity of the vestibulo-ocular reflex in the cat. *Ann.* NY Acad Sci 374:504–512

Suzuki JI, Cohen B (1964) Head eye body + limb movements from semicircular canal nerves. Exp Neurology 10:393–405

Suzuki JI, Goto K, Tokumasu K, Cohen B (1969a) Implantation of electrodes near individual vestibular nerve branches in mammals. Ann Otol Rhinol Laryngol 78(4):815–826

Suzuki JI, Tokumasu K, Goto K (1969b) Eye movements from single utricular nerve stimulation in the cat. Acta Otolaryngol 68(4):350–362

Trillenberg P, Shelhamer M, Roberts DC, Zee DS (2003) Cross-axis adaptation of torsional components in the yaw-axis vestibulo-ocular reflex. Exp Brain Res 148(2):158–165